Estuaries and Coasts
https://doi.org/10.1007/s12237-020-00732-1

SPECIAL ISSUE: SHALLOW WATER MAPPING

Impacts of 150 Years of Shoreline and Bathymetric Change in the Coos Estuary, Oregon, USA

E.F. Eidam[1] · D.A. Sutherland[2] · D.K. Ralston[3] · B. Dye[2] · T. Conroy[2] · J. Schmitt[4] · P. Ruggiero[5] · J. Wood[5]

Received: 29 April 2019 / Revised: 7 January 2020 / Accepted: 17 March 2020

Abstract

Estuaries worldwide have evolved over the past few centuries under development activities like dredging and shoreline reclamation, which commonly lead to increased channel depths and reduced intertidal areas. The Coos Estuary offers a useful example of how these changes, common to diverse global estuaries, have altered tidal and salt dynamics, with implications for estuarine habitats. In the past 150 years, the primary navigation channel has been deepened from ~ 6.7 to 11 m, generating a 12% decrease in estuary area and 21% increase in volume. To evaluate the present and future impacts on the Coos and similar estuaries, a hydrodynamic model was implemented using a detailed bathymetric dataset compiled from multiple data sources including agency charts, water-penetrating lidar, and single-beam-sonar small-vessel surveys. The model was then re-run using grids constructed from 1865 survey data and a future proposed dredging plan. Changes in the hypsometry from 1865 to present have driven a 33% increase in tidal amplitude, an 18% increase in salinity intrusion length, a doubling of the subtidal salt flux, and an increase in ebb dominance of currents. A proposed channel-depth increase from 11 to 14 m is predicted to generate a negligible change in tidal range and a small increase in the salinity intrusion length. These results highlight the utility of curating high-resolution bathymetric datasets for coastal management applications through modeling. The historical and modern models quantify how local bathymetric modifications can significantly alter tidal and salinity regimes and provide context for estuarine response to global climate-change drivers.

Keywords Estuary · Dredging · Habitat change · Hydrodynamics · Finite-volume model · Shoreline change · Sea-level rise · Sediment

Communicated by Mead Allison

Electronic supplementary material The online version of this article (https://doi.org/10.1007/s12237-020-00732-1) contains supplementary material, which is available to authorized users.

✉ E.F. Eidam
efe@unc.edu

[1] Department of Marine Sciences, University of North Carolina at Chapel Hill, 3202 Venable and Murray Halls, CB 3300, Chapel Hill, NC 27599, USA

[2] Department of Earth Sciences, University of Oregon, 100 Cascade Hall, Eugene, OR 97403, USA

[3] Applied Ocean Physics & Engineering Department, Woods Hole Oceanographic Institution, 266 Woods Hole Road, MS #11, Woods Hole, MA 02543, USA

[4] South Slough National Estuarine Research Reserve, P.O. Box 5417, Charleston, OR 97420, USA

[5] College of Earth, Ocean, and Atmospheric Sciences, Oregon State University, 104 CEOAS Administration Building, Corvallis, OR 97331, USA

Introduction

Estuaries are critical zones of human and ecosystem services (e.g., Martínez et al. 2007; Barbier et al. 2011; Guerry et al. 2012), and over the past ~ 150 years, many larger systems have been increasingly modified to accommodate port facilities, coastal protection, land reclamation, and other services. These uses often involve a substantial change to the bathymetry of the estuary, primarily through channel deepening, shoreline hardening, and reclamation of intertidal and shallow subtidal areas (sometimes as a result of dredge spoil disposal). For many systems, the result is a net decrease in estuary area and an increase in estuarine volume. For example, the Elizabeth River Estuary (Norfolk, VA) has been dredged for > 100 years to accommodate large ship traffic and has also seen land reclamation (especially during World War II) for port and airport facilities resulting in a ~ 25% reduction in area and ~ 270% increase in volume (Nichols and Howard-Strobel 1991). Boston Harbor has similarly seen 21 km^2 of land

reclamation since 1800, together with a near doubling of channel depth from ~ 8 to 15.5 m (Talke et al. 2018). These modifications result in bathymetric changes which can overshadow those driven by natural processes of sedimentation and sea-level change (van der Wal et al. 2002)—for example, the Mersey Estuary (England) volume increased by 0.1% per year due to dredging in the 1900s, as compared with an expected 0.02% per year increase driven by sea-level rise (Lane 2004).

These types of modifications impact the hypsometry and in turn the hydrodynamics and sediment dynamics of an estuary, sometimes with unintended consequences. In the Ems Estuary (Netherlands), channel deepening enhanced the estuarine circulation and amplified the tidal range, leading to a "hyperturbid" estuary and greater need for maintenance dredging (e.g., Talke et al. 2009; van Maren et al. 2015). In Elkhorn Slough (CA), reclamation of large marsh areas contributed to the transition of remaining marshes into erosional, intertidal mudflats (Van Dyke and Wasson 2005). Despite significant literature on estuarine dynamics that predicts changes to metrics such as salt intrusion length or subtidal exchange flow (MacCready and Geyer 2010) with channel deepening, numerous studies show counterexamples that contradict the theory. For example, a deepening of the channel in the greater Hudson River Estuary led to an increase in the salt intrusion length but no change in strength of the estuarine circulation (Ralston and Geyer 2019), while a similar deepening of Kill van Kull at the entrance to Newark Bay (New Jersey) resulted in the opposite effect of minimal change in salt intrusion length but a strengthening of the estuarine exchange flow (Chant et al. 2018). Increases in tidal amplitude (DiLorenzo et al. 1993; Jay et al. 2011; Winterwerp et al. 2013; Ralston et al. 2019) and storm surge (Familkhalili and Talke 2016) due to dredging and the associated decrease in effective friction have been noted in several estuaries, but in systems where river discharge events contribute significantly to the total water level, the net effect can be reduced flooding frequency (Ralston et al. 2019).

To effectively manage estuaries and understand the complex physical feedbacks related to changes in bathymetry and net volume, hydrodynamic and sediment transport models are often applied. These models require detailed, up-to-date bathymetric datasets. Because of the wide range of depths and turbid conditions found in a typical estuary, such datasets can be difficult to obtain using a single survey method like shipboard multibeam or airborne lidar. Where robust bathymetric datasets are available, historical data concerning changes in depths and physical conditions is particularly valuable for understanding changes in estuarine dynamics and subtidal habitats, but is often unavailable or dispersed among various archives. In this study, we took advantage of multiple existing new bathymetric datasets, historical sounding charts from 1865, and a proposed future dredging plan to (1) generate a robust joint bathymetric dataset to facilitate ecosystem management by local stakeholders; (2) characterize shoreline and bathymetric changes in the Coos Bay Estuary, Oregon for a period of > 150 years; and (3) implement 3D finite-volume hydrodynamic models for past, present, and future estuarine configurations, to determine how channel deepening has changed the tidal amplitude, salinity structure, and mechanisms of exchange in the estuary. The results demonstrate the utility of merging multiple bathymetric datasets into a high-resolution data product, in order to provide a 150-year context for hydrodynamic changes in the estuary and a present-day baseline assessment for managers navigating future developments. Because the intertidal losses and channel deepening in the Coos Estuary are representative of many systems worldwide, the results provide guidance for interpreting and understanding tidal and salinity shifts in the many estuaries subject to dredging and shoreline reclamation.

Regional Setting

Geology, Hydrology, and Climate

The Oregon coast is approximately 500 km long, extending from the mouth of the Columbia River in the north to the Klamath Mountains and the California border in the south. The rugged character of this coast results directly from its geologic setting, a tectonically active margin (e.g., Satake et al. 2003). Modern rates of relative sea-level rise in this region are strongly affected by tectonics with a local rate of 1.10 ± 0.73 mm/year, less than the global average (NOAA 2018; Komar et al. 2011). If this rate persists for the next 150 years, water levels in the estuary will increase by ~ 17 cm, a modest amount for a system like Coos Bay with steep relief.

The Coos Estuary (Fig. 1), located north of Cape Arago, is one of the largest estuaries on the US west coast with an area of 54 km^2, including ~ 50% intertidal flats (Rumrill 2006). The bay is horseshoe-shaped, reflecting the antecedent river valley that has flooded during sea-level transgression since the Last Glacial Maximum and an anticline located under the communities of North Bend and Coos Bay. A shallow side embayment called South Slough extends southward into a syncline near the entrance (Baker 1978). The main estuary has been heavily modified in the past ~ 150 years, while most of South Slough (south of the Charleston Harbor and bridge) has remained in a more natural state. Presently, 25 km^2 of the system is managed as a National Estuarine Research Reserve (NERR), a network of protected habitats managed for long-term research, education, and coastal stewardship.

The main channel of the estuary is ~ 11 m deep in the western reach, exclusive of a naturally deeper region immediately inside the entrance. The western reach has been deepened since the early 1900s from a depth of ~ 6.7 to ~ 11 m, to

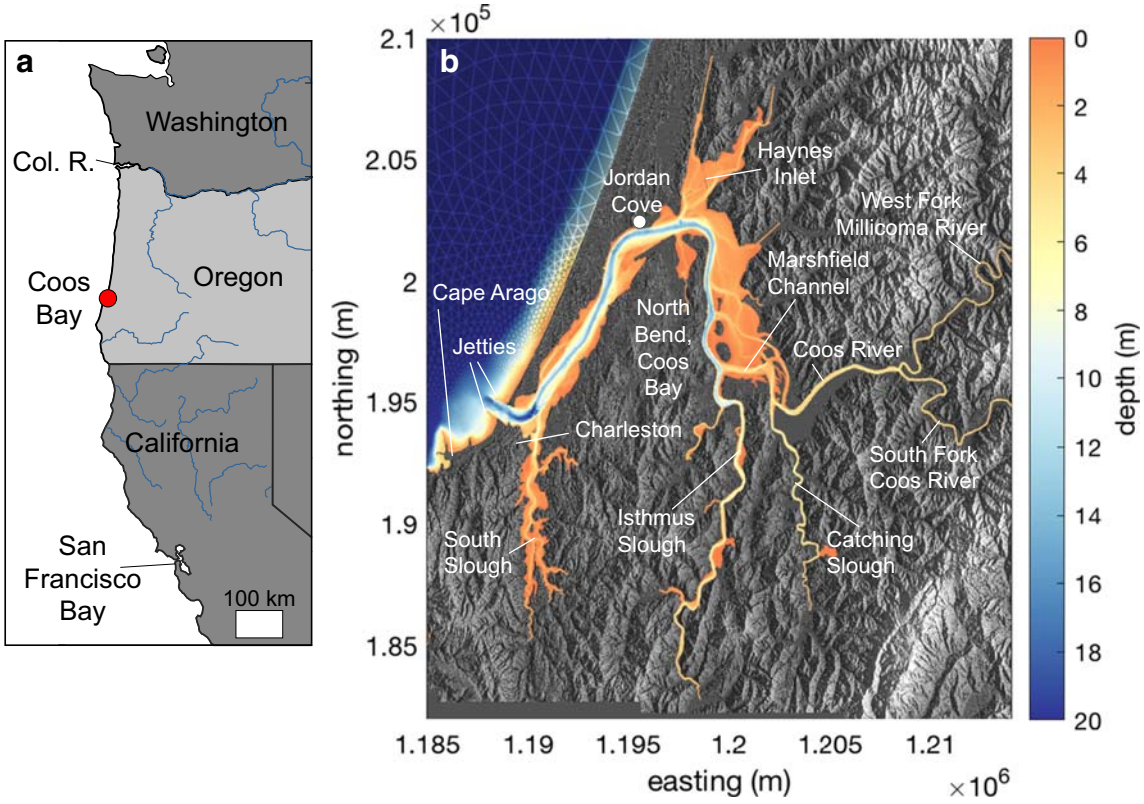

Fig. 1 Vicinity map. (a) Coos Bay is located on the south-central Oregon Coast and is the largest estuary between the Columbia River and San Francisco Bay. (b) Major tributaries and locales in the Coos Bay region. Lidar data are from www.oregongeology.org/lidar. Bathymetric product is from this study

accommodate vessel traffic to the Port of Coos Bay. Tides are mesotidal, mixed semi-diurnal, and currents average 1 m s^{-1} (Baptista 1989). The tidal prism is ~30% of the estuarine volume (Hickey and Banas 2003). Numerous rivers and creeks supply freshwater to the bay, including the Coos River, the largest source. Discharges range from ~1 m^3 s^{-1} during the summer low-flow season to >300 m^3 s^{-1} during winter storm peaks, which typically last several days. The system is partially to well-mixed in the summer and strongly stratified in the winter after rain events (Sutherland and O'Neill 2016). Although the discharge and salinity structure are highly seasonal, the estuarine exchange flow and landward salt flux are dominated by tidal processes that depend more on the spring-neap variability in tidal amplitude than the seasonal or event discharge forcing (Conroy et al. 2019).

Ecology and Management

The Coos Estuary comprises multiple sub-habitats including open water channels, tidal flats, tidal fresh and saltwater marshes, and forested swamps. This rich mix of environments supports numerous species which are commercially and recreationally important (Roye 1979), including crabs (e.g., *Cancer magister*, *Cancer productus*), bivalves (e.g., *Crassostrea gigas*, *Tresus capax*), fish (e.g., *Oncorhynchus kisutch*, *Platichythys stellatus*), and waterfowl (the Coos Estuary is centered along the Pacific Flyway). Ecologically or culturally important non-commercial species are also present, including mammals (e.g., *Phoca vitulina*, *Zalophus californianus*) and the Olympia oyster (*Ostrea lurida*), which re-established itself in the Coos Estuary after being naturally extirpated in the 1700s (Groth and Rumrill 2009).

Prior to Euro-American settlement of the area, the Coos Estuary supported several tribes that practiced subsistence-based hunting, fishing, food gathering, and trading. These activities were supplanted by Euro-American settlers by the mid-1800s who developed heavy extraction industries (coal, timber, agriculture, commercial fishing) and shifted the estuarine landscape (Caldera 1995). Stabilization of the bay mouth was initiated in the late 1880s, and by the end of the 1930s, jetties were established and large-scale channel and harbor deepening projects were completed to accommodate ship traffic to the port (Ivy 2015). During this era, marshes were also filled, diked, and drained, and forested wetlands were converted for agricultural use. By the 1960s, as much as 73–90% of the estuary's pre-industrial tidal areas were filled using channel material to provide residential, industrial, and agricultural land (Ivy 2015; Brophy 2017; Hoffnagle and Olson 1974). A robust commercial salmon fishery was in serious decline by the late 1980s (Ivy 2015), partially in response to logging practices of splash-damming, log rafting, storage cribs, and tideland reclamation.

Today, the Coos Estuary is shallow over most of its area (< 4 m deep in over half of the estuarine extent), has four tidal wetland types (seagrass, emergent marsh, scrub/shrub swamp, and forested swamp), and has a bed composed primarily of unconsolidated sediments (OCMP 2014). Industrial and commercial uses, while still common, have declined in the past few decades, while recreation and tourism industries have expanded—especially for recreational fish and shellfish harvesting and kayaking.

In 1973, Oregon created a legal framework for land-use planning intended to balance natural resource protection with land-use needs. Natural resource inventories were developed shortly thereafter for each major estuary in Oregon. The Coos Bay Estuary Management Plan was adopted in 1986 and sets the development and protection guidelines for the Coos Estuary, which was designated a deep-draft development estuary. However, this estuarine management plan has not been updated since its adoption, despite significant physical and cultural changes to the region, as well as technological advances in mapping and understanding of the estuary. In addition, planning for future change in the estuary is underway: an example is the proposed deepening and widening of the main channel to accommodate access for larger ships to a proposed liquid natural gas terminal at Jordan Cove (Fig. 1). Results from this study will in part provide new management tools for regional communities, including more comprehensive, high-resolution bathymetric data; shoreline change analyses dating from 1865 to present; and model hydrodynamics to help forecast future conditions. The results also provide a broadly applicable case study in how anthropogenic modifications to the hypsometry (toward a deeper system with less intertidal area), which are common to many estuaries worldwide, can significantly impact tidal amplitude and salinity distribution.

Methods

Shoreline and Bathymetric Digitization from Historical Maps

Twelve bathymetric charts of Coos Bay from 1865 to 2011 were downloaded from NOAA (historicalcharts.noaa.gov; NOAA 2019b). Maps were imported to ESRI ArcGIS and georeferenced. Maps from 1927 and later were referenced using latitude/longitude points on the map according to the datums given (Table S1). Maps prior to 1927 were georeferenced by hand using bedrock features mapped to the modern NOAA shoreline layer, which was transformed into the NAD1927 datum.

Shorelines were traced by hand within ArcMap for all maps shown in Table S1. Estuary areas were then calculated from the shoreline polygons (Fig. 2) for each map after transformation to the Oregon State Plane NAD83 datum. For regions beyond the historical chart extents (e.g., southern portion of South Slough, northern portion of Haynes Inlet, and the southern parts of Isthmus and Catching sloughs), the modern shorelines were used to supplement the historical shorelines, based on the assumption that little modification and little change have occurred in these shallow regions that have poor navigability and minimal shoreline infrastructure.

Historical bathymetric data were digitized from the 1865 map, which pre-dated construction of the jetties. Discrete depth soundings were marked by hand, and contours representing the shoreline, intertidal line (0-m contour), 6-ft (1.8-m) contour, and 8-ft (2.4-m) contour were traced and then converted to discrete points within ArcMap. Because historical depths were referenced to "average lowest low water," a 1.24-m depth offset was added to convert to mean sea level (MSL) based on the modern offset between MSL and mean lower low water (MLLW) at the North Bend tidal station (NOAA 2019a). Digitized bathymetric points were interpolated onto a historical model grid, as discussed in the "Hydrodynamic Modeling" section, for use in the hydrodynamic model. It should be noted that the historical maps did not provide elevation data for the shallow (un-navigable) portions of the tidal flats on the east side, and thus these regions received interpolated depths of 1.24 m based on adjacent intertidal lines (corrected for the offset between MLLW and MSL). Because the survey charts excluded the upper reaches of South Slough and Haynes Inlet, modern bathymetric values were used for these regions, based on the same shoreline assumptions described above.

When digitizing historical charts for shoreline locations and bathymetry, primary sources of error include the map resolution (e.g., line thicknesses) and errors (vertical and horizontal) in reported depths. Depths on historical charts are commonly rounded to integer values and are generated by different survey methods depending on the time period (e.g., lead-lining versus modern sonar surveys; Jakobsson et al. 2005). Based on the resolution and line widths of the historical maps, we estimated that shoreline locations were within ± 5 m of the actual locations. If we approximate the area of the estuary to be a 1-km-wide rectangle, the length would be equal to the area in Table S1 multiplied by 1/km. These lengths are roughly equal to the length of the estuarine channel from the end of South Slough to the end of Isthmus Slough plus the length of Catching Slough, i.e., a reasonable approximation given the scale of the estuary. An offset of ± 5 m would yield a variation of ± 1% of the total area, a relatively minor amount. For the bathymetry, we applied the method of Jakobsson et al. (2005) to evaluate errors: point-wise differences in elevation between raw digitized depths and an interpolated triangulated bathymetric

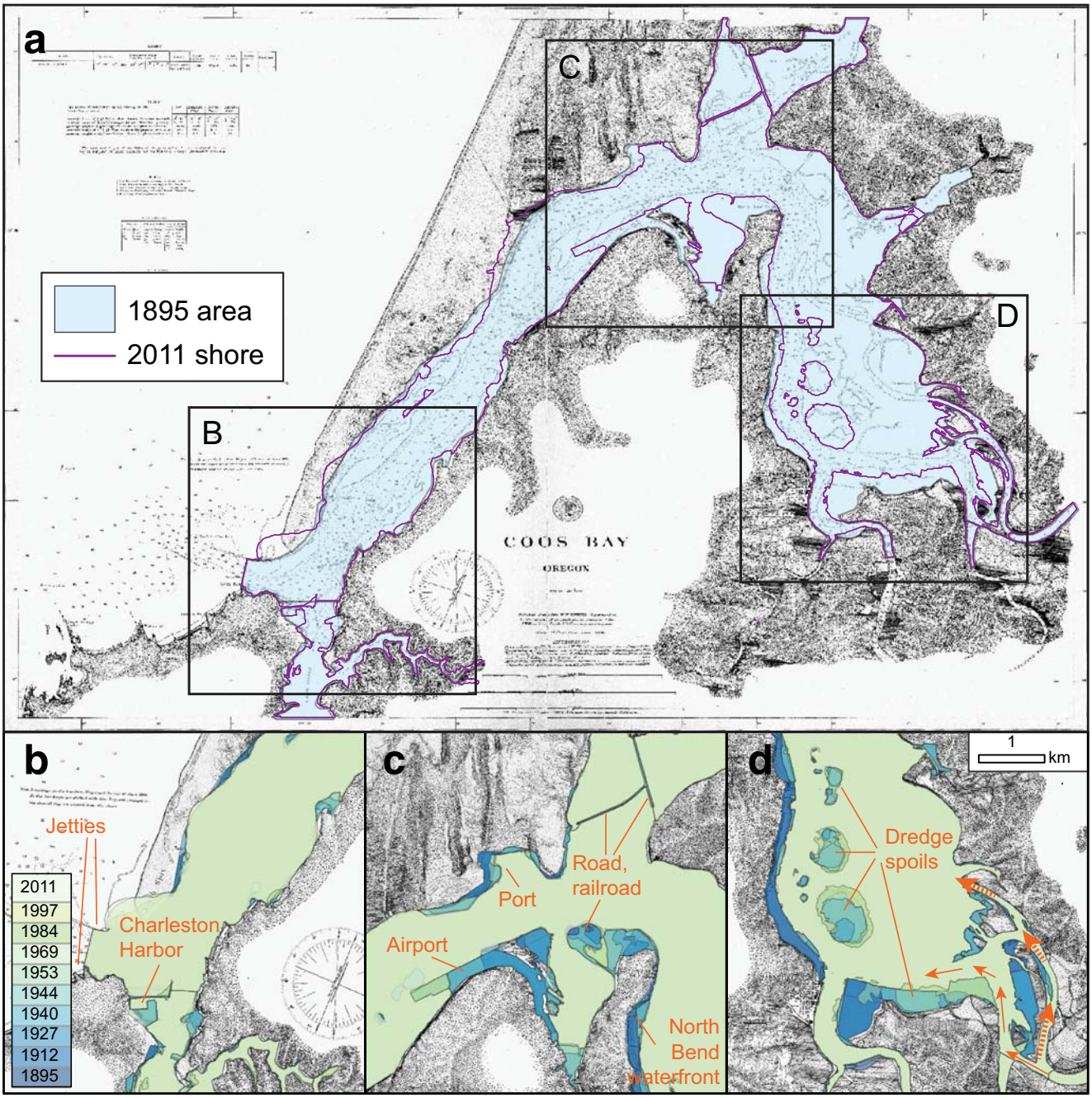

Fig. 2 Shoreline change. (a) An example Coast Survey bathymetric chart from 1895, with modern shoreline overlay, highlighting areas of change in the estuary (chart from NOAA 2019b). (b) Detail of Charleston Harbor construction. (c) Detail of land reclamation associated with transportation and shipping projects. (d) Detail of dredge spoil dumping areas and re-routing of the Coos River channel (former path is in dash arrows; present path is in solid arrows). See Bartlett (2018) for additional details

mesh were computed in MATLAB. In our analyses, we subsampled depth points that were within 5 m horizontally of a triangular node to reduce offset errors. The mean difference between the raw data points and gridded points (n = 1035) was − 1.9 cm, meaning the gridded depths tended to be slightly greater than the raw digitized points. This offset represented a ~ 2% error for depths on the order of 1 m and 0.2% error for depths on the order of 10 m.

Mapping the Modern Estuary

To create a modern bathymetric dataset, we combined several recent datasets (Table 1) into one non-overlapping dataset. An existing 1/3 arc second DEM provided by NOAA (Carignan et al. 2009) provides bathymetry data for the continental shelf offshore of the estuary. The newly created bathymetry included data from a water-penetrating airborne coastal lidar gridded

Table 1 Data sources used to compile present-day bathymetry. All data were converted to the NAD83 horizontal datum and mean sea level (MSL) vertical datum in the final merged bathymetric product, which is available at https://github.com/das7105/Coos-Bay-Bathymetry.git. Source data coverage is shown in Fig. S1

Source	Date(s) collected	Resolution	Horizontal datum	Vertical datum
USACE lidar[a]	2014	1 m	Geographic NAD83	NAVD88 (m)
USACE channel surveys[b]	2017, 2018	< 1 m	OR State Plane NAD83	MLLW (ft)
NOAA Port Orford DEM[c]	2009	1/3 arc second[d]	Geographic WGS1984	MHW (m)
Single-beam sonar (CPS)[e]	2017, 2018	< 1 m	OR State Plane NAD83	NAVD88 (m)
ODFW SEACOR[f]	2017	< 1 m	Geographic WGS1984	MLLW (m)

[a] Coastal lidar flown over portion of Coos Bay, data: https://coast.noaa.gov/htdata/lidar1_z/geoid12b/data/4905/

[b] Annual channel surveys, data: https://www.nwp.usace.army.mil/Missions/Navigation/Surveys/

[c] Date, data: https://data.noaa.gov//metaview/page?xml=NOAA/NESDIS/NGDC/MGG/DEM/iso/xml/410.xml&view=getDataView&header=none#

[d] 1/3 arc second is roughly 10 m at this geographic location

[e] Collected as part of this study, see description in text

[f] Oregon Dept Fish & Wildlife, shallow multibeam data, https://www.dfw.state.or.us/mrp/shellfish/seacor/

at 1-m spacing along with annual channel surveys from the US Army Corps of Engineers. These datasets did not extend into the narrow sloughs and tidal flats of the upper estuary and Sough Slough, so we collected shallow water bathymetric surveys using the coastal profiling system (CPS; Ruggiero et al. 2005), a high-speed maneuverable personal watercraft-based system.

The CPS consists of a single-beam echo sounder, survey-grade GPS receiver and antenna, and an onboard computer system running the Hypack hydrographic survey software. This system is capable of measuring water depths from ~ 0.5 to ~ 50 m, with bathymetric data collected at a GPS sample frequency of 10 Hz. The survey-grade GPS equipment have manufacturer reported RMS accuracies of approximately ± 3 cm + 2 ppm of baseline length (typically 10 km or less) in the horizontal and approximately ± 5 cm +2 ppm in the vertical in a real-time kinematic (RTK) surveying mode. These reported accuracies are, however, additionally subjected to multi-path errors, satellite obstructions, poor satellite geometry, and atmospheric conditions that can combine to cause a vertical GPS drift of as much as 10 cm. Survey data (Fig. S1) were collected in spring over 2 years (2017 and 2018) using the Oregon Real-Time GPS Network (ORGN), a network of permanently installed, continuously operating GPS reference stations. Obviously bad, or noisy, data attributed to echo sounder dropouts or poor returns (common while collecting data in shallow depths and turbulent environments) or contamination of the bottom return by eelgrass beds were eliminated from the data record. A smoothing operation was performed to eliminate scales of morphological variability difficult to resolve, the value of which was influenced by the pitch and roll of the CPS vessel from wave activity and wind chop.

A final, merged bathymetric dataset (including all data listed in Table 1) was created by combining the available datasets such that the combined elevations were not overlapping in space. For areas where limited bathymetric data existed such as in the upper reaches of smaller channels, a linear along-channel slope with uniform across-channel depth was prescribed. Combined points were interpolated onto the model grid.

Volumes were calculated based on MSL vertically referenced to the Charleston NOAA tide station (tidesandcurrents.noaa.gov, station 9432780). Volume changes were determined by comparing the interpolated, gridded bathymetric products for the 1865 case, the present case, and the future proposed dredging case. The estuary regions were defined from the entrance (bounded by jetties in the modern case) to the confluence of the West Fork Millicoma River and South Fork Coos River (see Fig. 1), and all sloughs and side embayments were included.

Hydrodynamic Modeling

We simulated hydrodynamics within the Coos Estuary using the finite-volume coastal ocean model (FVCOM v3.2.1; Chen et al. 2003). FVCOM utilizes a finite-volume discretization of the three-dimensional, hydrostatic, primitive equations on an unstructured grid, allowing high resolution in the main channels (15-m horizontal spacing) and coarser resolution in the coastal ocean. In light of significant shoreline changes (Fig. 2), two grids were created with slightly different shorelines (Fig. 4a, b): one for the historic, pre-dredging scenario and second for the present-day and future (proposed/dredged) scenarios. These grids have similar resolution within the estuary and total number of triangular elements (historic ~ 191,500; present and proposed dredging ~ 195,000). FVCOM allows wetting and drying of grid cells to accommodate representation of tidal water-level fluctuations, and the minimum wet cell depth was set to 0.4 m. For all simulations, the k-ε turbulence closure scheme (Umlauf and Burchard 2003) was

employed with twenty sigma layers in the vertical. All other model parameters are described in detail in Conroy et al. (2019).

Model boundary conditions included river discharge at fourteen locations within the estuary, tidal forcing at the open boundary (TXPO Tidal Model Driver; Egbert and Erofeeva 2002), and salinity at the open boundary from a regional ocean model (Giddings et al. 2014). Most freshwater enters the estuary through the Coos River (composed of S. Fork Coos River, W. Fork Millicoma River, E. Fork Millicoma River, and Marlow Creek), which is the only gaged freshwater input to the estuary. We scaled the freshwater input from the remaining smaller creeks based on the relative watershed area. Conroy et al. (2019) extensively validated the performance of the present-day model setup, showing that over a year-long simulation, the model had considerable skill at replicating sea level at tidal and subtidal timescales, the salinity structure of the estuary, and both tidal and subtidal currents.

For this study, we leverage the validated model setup (Conroy et al. 2019) to build a tool to explore how historical and future changes to geometry and bathymetry affect estuarine dynamics. For each geometry and bathymetry combination (historic, present, and proposed future dredging cases), we ran two idealized discharge scenarios that represented the dominant seasonal shift in forcing from low-flow conditions of summer to the event-driven, higher discharge conditions of winter (Table S2). For summer, we set the Coos River discharge to a steady 1 $m^3\ s^{-1}$, while for winter, we set a baseline flow of 20 $m^3\ s^{-1}$ with a storm event peaking at 200 $m^3\ s^{-1}$ over a 2-day ramp-up period. The peak discharge coincided with spring tides and ramped down over several days before returning to baseline flow. This discharge event was also run for a period of neap tides, and because the results were similar to those of the spring case, they have been omitted for brevity. We initialized each run from average summer and winter conditions taken from the realistic hindcast (Conroy et al. 2019), running each for a total of 2 months. Mean fields were developed as averages over the entire 2-month period.

To compare tidal amplitudes, ebb dominance, and salinity distributions between the two cases, we calculated mean values over a 58-day period for each model run. To assess ebb dominance, we computed the ratio $(u_{ebb}/u_{flood})^3$, where ratios greater than 1 indicate ebb dominance and the cubic power comes from the statistical definition of skewness and serves as a useful scaling for net sediment transport direction (e.g., Nidzieko and Ralston 2012). Tidal amplitudes were computed using the T-Tide analysis software (Pawlowicz et al. 2002) and represent the sum of the 35 tidal components. We also decomposed the salt flux using the classical decomposition (Fischer 1976; Lerczak et al. 2006; Ralston et al. 2010). The total salt content (S) in the estuary (dS/dt) depends on a balance between export by the advective barotropic river flux (F_R) pushing salt out of the estuary and import by the spatial correlations in salinity and velocity at subtidal time scales, due to processes such as gravitational circulation and the mean stratification (F_{Eul}) and the spatial and temporal correlations at tidal time scales, representing the tidal oscillatory salt flux (F_T) that generally transport salt landward. We calculated the terms in this unsteady salt balance at cross-sections in the model simulations as $dS/dt = F_R + F_{Eul} + F_T$ (Conroy et al. 2019).

Results

Shoreline Changes

Between 1865 and 2011, the estuary area decreased 12% from 57.8 to 51.0 km^2 (Figs. 2, 3). These results exhibit a similar trend as noted in an analysis of maps from 1863, 1916, and 1953 by Borde et al. (2003). The greatest change occurred between ~ 1910 and 1970, at an average rate of − 0.11 km^2 per year (or 0.19% per year relative to the 1865 area). The most notable shoreline changes included

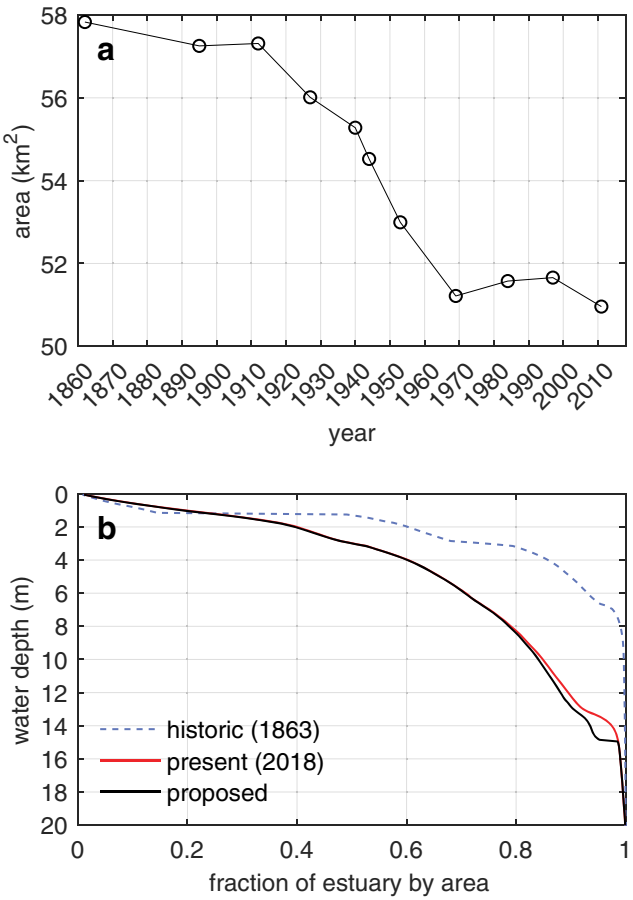

Fig. 3 Changes in estuarine area and water-depth distribution. (a) Area change between 1865 and 2011; substantial change occurred between approximately 1910 and 1970. (b) Hypsometric curves of the historic, present, and proposed estuary bathymetry

construction of a jetty near Charleston (completed by 1914), construction of the airport and constriction of Pony Slough (1940s), construction of the Charleston Harbor (1950s), and dumping of dredge spoils on the east intertidal flats and south side of Marshfield Channel (between the 1930s and 1970s). The airport at North Bend was constructed between 1944 and 1953, and the runway was extended around 1992. Additional smaller shoreline changes occurred adjacent to the towns of Coos Bay (starting prior to 1898) and North Bend (starting around 1908) due to construction of port facilities. Some changes in channel island configuration occurred in the main channel on the west side. Shorelines on the east side of the bay and in South Slough were generally stable. In Haynes Inlet, two causeways were constructed on the shallow flats, and flow was constricted to two deep channels preserved under bridges. Many of the shoreline changes resulted in a decrease in estuary width, e.g., from 1.2 to 0.75 km near the airport (Fig. 2c, Table S1).

Substantial modifications were also made at the estuary inlet. Jetties were constructed in the mid-1800s, reducing the opening width from 1.3 to 0.62 km. In the upper estuary, the Coos River was re-routed from a primary channel that discharged onto the eastern intertidal flats into a new primary flow path of Marshfield Channel between 1940 and 1944. This diversion was constructed to support port facilities near the entrance of Catching Slough (Figs. 1, 2d).

Bathymetry Changes

The total volume of the estuary increased from 1.39×10^8 in 1865 to 1.68×10^8 m^3 at present, a +21% change. This change was disproportionate between shallow and deep areas (Figs. 3b, 4). Regions < 4 m deep decreased in volume from 7.74×10^7 to 5.26×10^7 m^3 between 1865 and present (Fig. 3b). In terms of area, this represented a shift from 86 to 60% of the total estuary. At the entrance, the thalweg was deepened and widened, while the shallow flats on the north side were filled to accommodate the north jetty. As a result, the cross-sectional area of the entrance nearly doubled from ~ 4230 to ~ 8120 m^2. The proposed future dredging would further increase the cross-section at the mouth to 8460 m^2 (Figs. 5, S2). Just inside the entrance at section B (Figs. 4, 5), the primary channel migrated northward. For the remainder of the thalweg leading to Isthmus Slough and Marshfield Channel (e.g., sections C through G), the channel experienced little lateral translation but was deepened from natural depths of ~ 3.4 to 7 m to new depths of ~ 4.5 to 15 m. In Marshfield Channel (section H), the channel was re-contoured but not necessarily deepened. Isthmus Slough was dredged from depths of ~ 7 to new depths of 11 m for a distance of ~ 1.5 km.

The expansive intertidal and subtidal flats on the east side of the estuary were not labeled with discrete depth soundings in early bathymetric charts, but the channels dissecting the flats appear to have been somewhat stable over time. A shallow channel extending northwest from the natural outlet of the Coos River appears to have filled slightly, and a few minor drainage channels were buried by dredging spoils (Fig. 2a). South Slough experienced limited dredging and deepening near the harbor; it is unknown if the bathymetry up-estuary of the historical map limits has changed significantly in the past century.

Under the proposed channel modification project, the main channel would be deepened to ~ 15 m below MSL from the estuary mouth to Jordan Cove, 14-km up-estuary (Fig. 4b, indicated by dashed line). The channel would also be widened by ~ 45 m (a 50% increase from present day). These modifications would increase the estuarine volume by 3.3% beyond present day.

Changes to Hydrodynamics and Estuarine Structure

Tides and Currents

The tidal amplitude throughout the estuary increased from the historical time period to the present day (Fig. 6a). For the present-day bathymetry, the tidal amplitude increases from ~ 2.1 m at the mouth to a maximum of 2.5 m near the entrance to Marshfield Channel (23 km). From there to the entrance of the Coos River (26 km), it decreases slightly (~ 0.1 m) and then increases again along the Coos River (Fig. 6a). The trend for the historical case is opposite, with an overall decrease from the maximum amplitude of ~ 2.1 m at the mouth to a minimum of ~ 1.4 m at the entrance to the Coos River. This trend includes a large drop (30% of total amplitude) across Marshfield Channel (Fig. 6a). The mean tidal amplitude increased by 33% in the present day compared with the historical case. The future dredged scenario shows a small change compared with present day, decreasing by 1.5% along the main channel and in South Slough (Fig. 6a). It should be noted that these changes do not necessarily imply greater water levels at high tide—the change in amplitude is generally manifested as lower water elevations during low tides in the present than in the past, relative to MSL.

Maximum mean ebb tidal currents generally decreased up-estuary for all cases, except in Marshfield Channel and/or the entrance to the Coos River, where currents reached local maxima (Fig. 6B). In the historical case, maximum ebb currents peaked at ~ 2.2 m/s near the entrance and decreased to ~ 0.2 m/s at 26 km, before reaching a local maximum of ~ 1.7 m/s at 27–29 km. A similar trend was observed in the present case, but maximum currents near the entrance were slower (~ 1.3 m/s) and two local maxima occurred at ~ 24 km and 27–29 km.

The tidal asymmetry (i.e., magnitude and duration of flood versus ebb tidal currents) also changed from the historical to present case, resulting in a generally more ebb-dominant system at present, despite the overall decrease in maximum ebb tidal

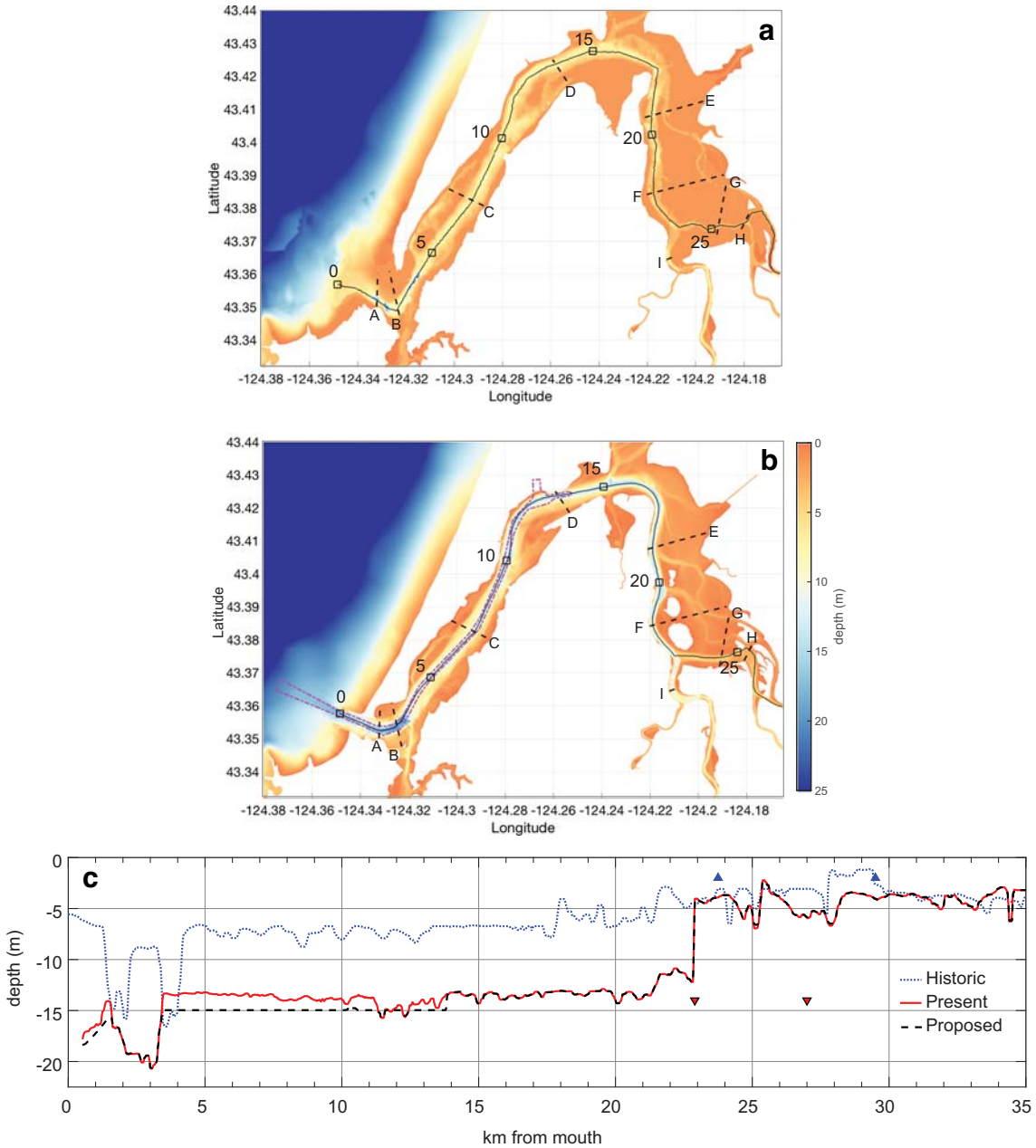

Fig. 4 (a) Bathymetry created for historical scenario with an along-estuary transect delineated (black line) with distances marked by a square every 5 km. Across-estuary transects (black dashed lines) are lettered A–I for use in Fig. 5. (b) Same as in A but for the present-day bathymetry. The proposed dredging will occur inside the magenta outline. (c) Bathymetry along the transects indicated in A and B, going from the mouth up the Coos River. The entrances to Marshfield Channel (seaward triangle) and the Coos River channel (landward triangle) in both historical (blue) and present/future (black/red) cases are shown

currents (Fig. 6b, c). At present, the estuary is moderately ebb dominant from the mouth to the bend at 17 km, with a $(u_{ebb}/u_{flood})^3$ ratio of 1.7. Farther up-estuary in Marshfield Channel and the Coos River entrance, the ratio increases to 10 with a small spatial-scale peak > 100. The fastest time-averaged currents (over the 58-day model period) occur at the mouth (1.2 m/s) and in Marshfield Channel (1.5 m/s). In the historical case, the maximum time-averaged ebb currents were generally larger (up to 2.2 m/s near the entrance and decreasing up-estuary) but were ebb dominant only within 4 km of the entrance (ratio = 4.4). In the remainder of the estuary, the historical ebb/flood ratio was ~ 1, except in Marshfield Channel where the currents were strongly ebb dominant.

Salinity Structure

Salinity decreases up-estuary, but vertical and horizontal gradients are strongly controlled by seasonal variations in river

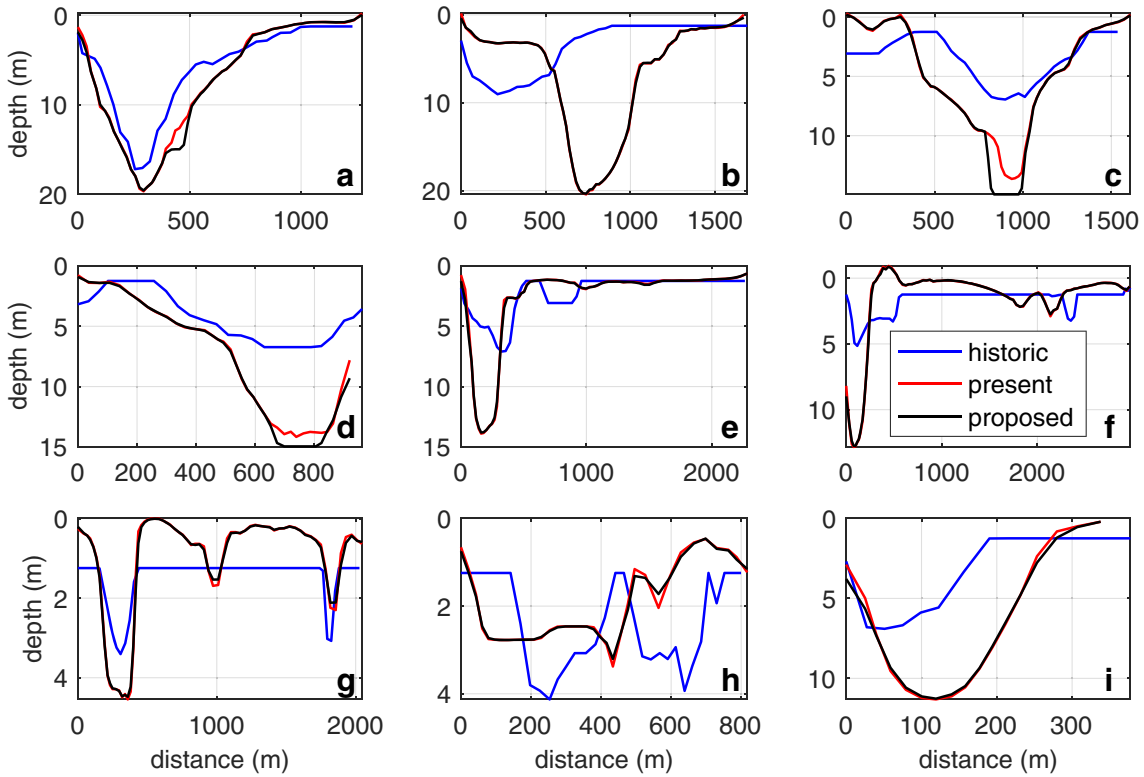

Fig. 5 Across-estuary bathymetric transects for historical (blue), present (red), and proposed (black) scenarios for transects labeled A–I in Fig. 4. Note the axis scales change between panels. The horizontal lines in Fig. 5 g, h, and i are artifacts of the assumed tidal-flat depths in regions of no data from the historical charts

discharge and deepening of the main channel between the historical and modern and future proposed dredging cases. Salt dynamics are summarized in Figs. 7 (main estuary) and 8 (South Slough). In general, the estuary gains salt in the summer during low-flow conditions and loses salt during winter high-flow conditions and storm events (Figs. 7a, 8a). During the summer low-flow season, the estuary is well-mixed (Figs. 9, S2) with average salinity in Marshfield Channel (23 km; Fig. 7a) near oceanic values (> 28 psu) and > 25 psu on average throughout most of South Slough (Fig. 8a). During the winter, the oceanic salinities shift down-estuary to within one tidal excursion of the mouth (i.e., at 5–10 km; Figs. 7, 9).

The mean salinity in the estuary has generally increased over time, especially in the upper estuary and during winter high-discharge events. Mean along-channel salinity increased ~ 1–2 psu from the historical to modern case for most locations, and salinity would increase an additional ~ 0.5–3 psu for the proposed dredging case (Fig. 7a). The lower estuary presently has less high-salinity water (> 31 psu) but experiences longer periods of inundation by intermediate salinity water than in the past (e.g., 23–30 psu; Fig. 7b)—hence the net increase in temporally averaged salinity. In the upper estuary, mean salinities have also increased, through longer periods of intermediate salinity (11–25 psu) (Fig. 7c).

South Slough has experienced an even greater net increase in salinity between the historical and modern conditions. In the modern case, salinities have increased by up to 15 psu in the wintertime and 7 psu in the summertime compared with the historical conditions (Fig. 8a), with the greatest changes occurring in the upper estuary (at 8–13 km). Salinity gradients and stratification have decreased (Figs. 9, S2), though the salinity in South Slough remains very tidally dependent, as evidenced by the wide range of values over a 2-month period (Fig. 8b, c).

Salinity intrusion length in the main estuary for high-discharge case increased ~ 18% in the modern estuary compared with the historical case (Fig. 7). The mean 2-psu isohaline for the winter forcing case was historically located at 27 km, but due to the more meandering channel and greater thalweg length for the historical bathymetry, this location is equivalent to ~ 25.5 km in the modern case. At present, the 2-psu isohaline is located at 30.5 km, representing a 5-km up-estuary translation as a result of dredging and other bathymetric modifications. In the future proposed dredging case, the salinity intrusion length increases to 30.6 km, representing little change in bottom salinity beyond the modern case. However, the range of salinities experienced at a given location is forecasted to shift toward higher salinities with the proposed dredging (Fig. 7b, c). In South Slough, the salinity intrusion length has also increased between past and present, exemplified by isohalines translating

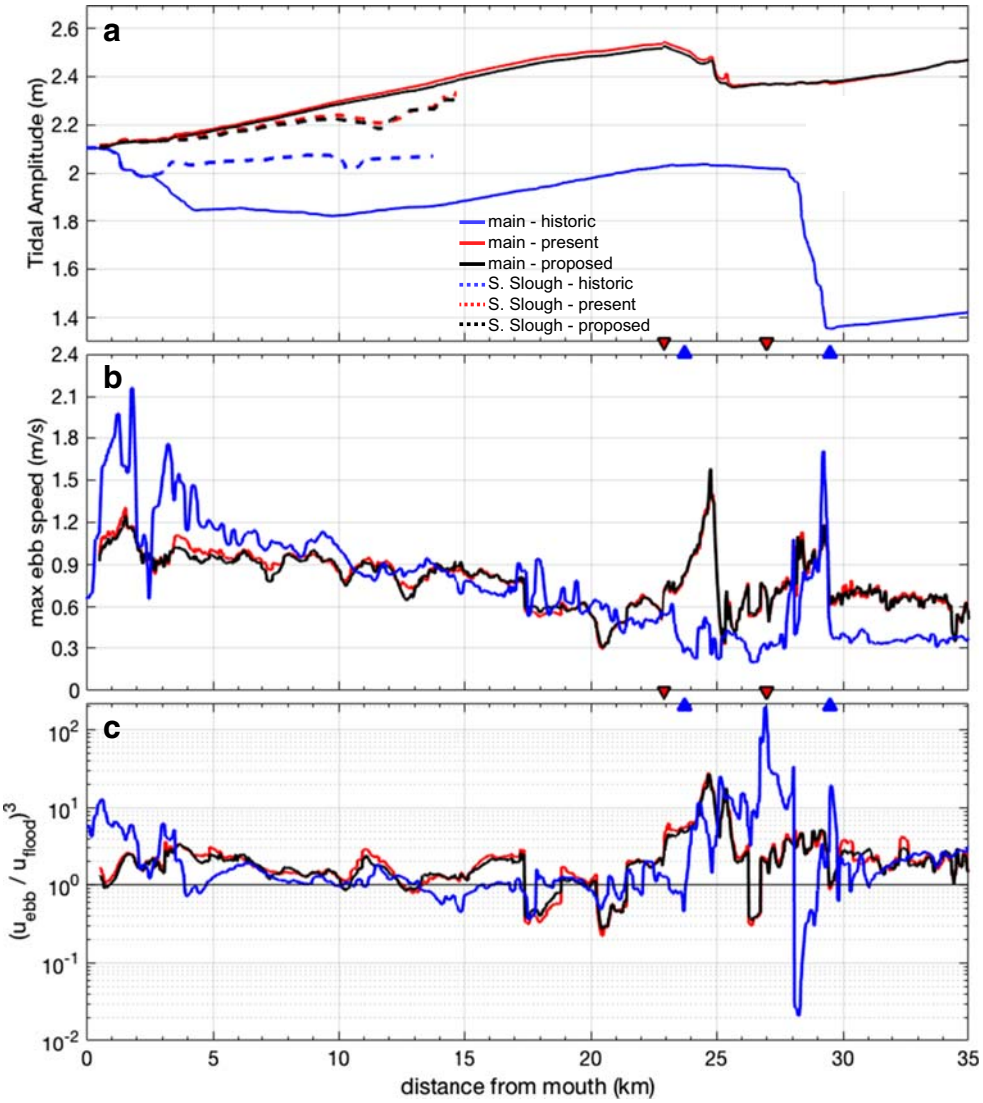

Fig. 6 (a) Total tidal amplitude along estuary for the three geometries, going from the mouth (0 km) to Marshfield Channel (first colored triangle) and into the Coos River channel (second colored triangle). Note that distances differ slightly between historical and present due to change in thalweg (see Fig. 4). Dashed lines show along-estuary transect up South Slough. (b) Same as in a, but for time- and depth-averaged maximum current speed during ebb tides at each along-estuary location going up the Coos River channel section. (c) Same as in b, but for the cube of the ratio of mean ebb current magnitude (u_{ebb}) to flood current magnitude (u_{flood}). Note the log scale for the *y*-axis

up-estuary by 2 km or more (Fig. 8a, S2). An additional up-estuary translation of a few hundred meters to ~1 km is forecasted for the proposed dredging case (Fig. S2), which will result in a larger percentage of time exposed to the higher salinity classes than in the present (Fig. 8b, c).

The shifts in salinity intrusion length and structure were associated with changes in the mechanisms of salt transport in the estuary. In the present geometry under the winter discharge conditions, the flux of salt into the estuary is primarily accomplished by tidal processes (F_T; Fig. 10a), and that is balanced by flux out of the estuary due to the river flow (F_R). The subtidal gravitational component (F_{Eul}) of the landward salt flux is about half that or less than the tidal component along most of the estuary, until near the entrance to Marshfield Channel where the terms are small and of similar magnitude (Fig. 10a). The fraction of the total salt flux due to tidal oscillations (F_T/F_T+F_E) was defined as ν by Hansen and Rattray Jr. (1965, 1966). For the present bathymetry case, the average value of ν seaward of Marshfield Channel is 0.6, reflecting the dominance of the tidal term. Similar results are found under the summer low discharge scenario, with the dominant balance between F_T and F_R extending over a larger region with the greater salinity intrusion. Conroy et al. (2019) showed the dominance of F_T over a year-long run with observed river discharge and the present-day geometry and also noted the central importance of the unsteadiness term (dS/dt, not shown in Fig. 10a) during all seasons in this type of estuary. That unsteadiness term is less important in this analysis because we are taking averages of the salt flux terms over the 2-month simulations.

In the historical and future proposed dredging cases, the salt flux terms have broadly similar trends, but with some notable differences (Fig. 10a). For the shallower historical bathymetry, the tidal salt flux term accounted for an even greater fraction of the total landward salt flux, with an average value for ν of 0.8. Between the historical and present cases,

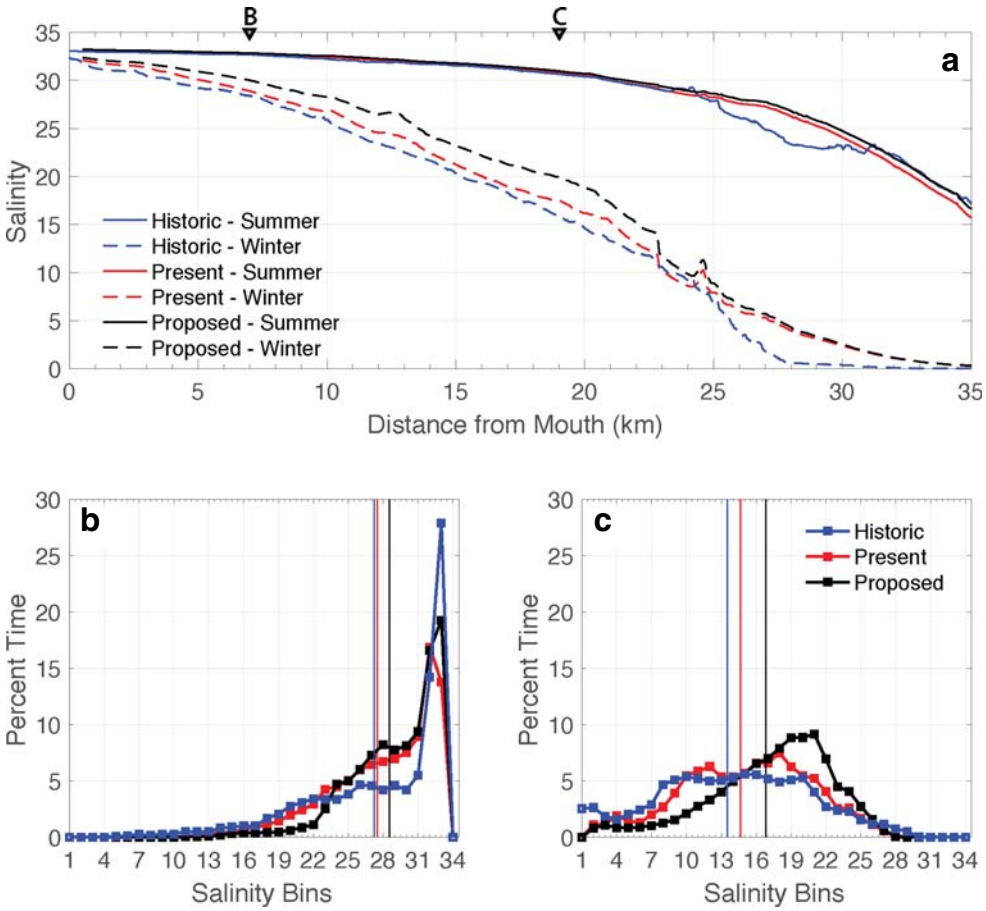

Fig. 7 (a) Time-averaged bottom salinity along a thalweg transect going from the estuary mouth up the Coos River for the six simulated scenarios. Triangles indicate locations for panels (B) and (C). (b) Percent time within a certain salinity class for only the winter high-flow scenario at the along-estuary location (7 km) indicated in (a) for each bathymetry. Solid vertical lines show the mean salinity for each bathymetry (color) at that location. (c) Same as in (b), but for a location 19 km along estuary, as indicated in panel (a)

F_{Eul} more than doubled over much of the dredged region of the estuary (Fig. 10b). F_T decreased, but less than the increase in F_{Eul} such that total landward salt flux increased, consistent with the increased salinity intrusion in the present case. The proposed dredging case results in additional increases in F_{Eul} of 50–100% over much of the affected region compared with the present bathymetry case, with only a small decrease in F_T (Fig. 10b). As a result, the tidal dispersive fraction of the salt flux ν decreases to an average of 0.5 in the proposed dredging case.

Characterizations of Suitable Habitat

The modern, high-resolution bathymetric dataset provides a useful tool for assessing potential eelgrass habitat. Areas ranging from 0.5 above MLLW to 1.0 m below MLLW have been identified as potential areas for eelgrass growth, based on light requirements in the Pacific Northwest (Thom et al. 2008). The new bathymetric dataset was used to assess the area of potential habitats in South Slough and the main estuary based on this range. For South Slough, depths were computed relative to MSL using the 1.24-m offset between MSL and MLLW from the Charleston tide station (station 9432780, tidesandcurrents.noaa.gov). For the main estuary, the 1.42-m offset from North Bend was used (station 9432895). Potential habitat areas comprised 13 km^2 of the main estuary and 1.9 km^2 of South Slough (Fig. 11). These habitats are dominantly located on shallow tidal flats but also occur along all major channels.

Discussion

In Coos Bay, the comparison of historical bathymetric charts with merged modern bathymetric datasets has revealed a characteristic deepening in the hypsometry of the estuary related to dredging and dumping of dredge spoils in shallow intertidal areas. Here, we discuss the details of these changes to highlight which portions of the estuary were most impacted on a local scale and use results from the hydrodynamic modeling to address how conditions throughout the estuary have changed in terms of tidal dynamics and salinity distribution.

Drivers of Shoreline and Bathymetry Change, 1865–Present

Over the past 150 years, Coos Bay has experienced many changes common to estuaries serving as port facilities and

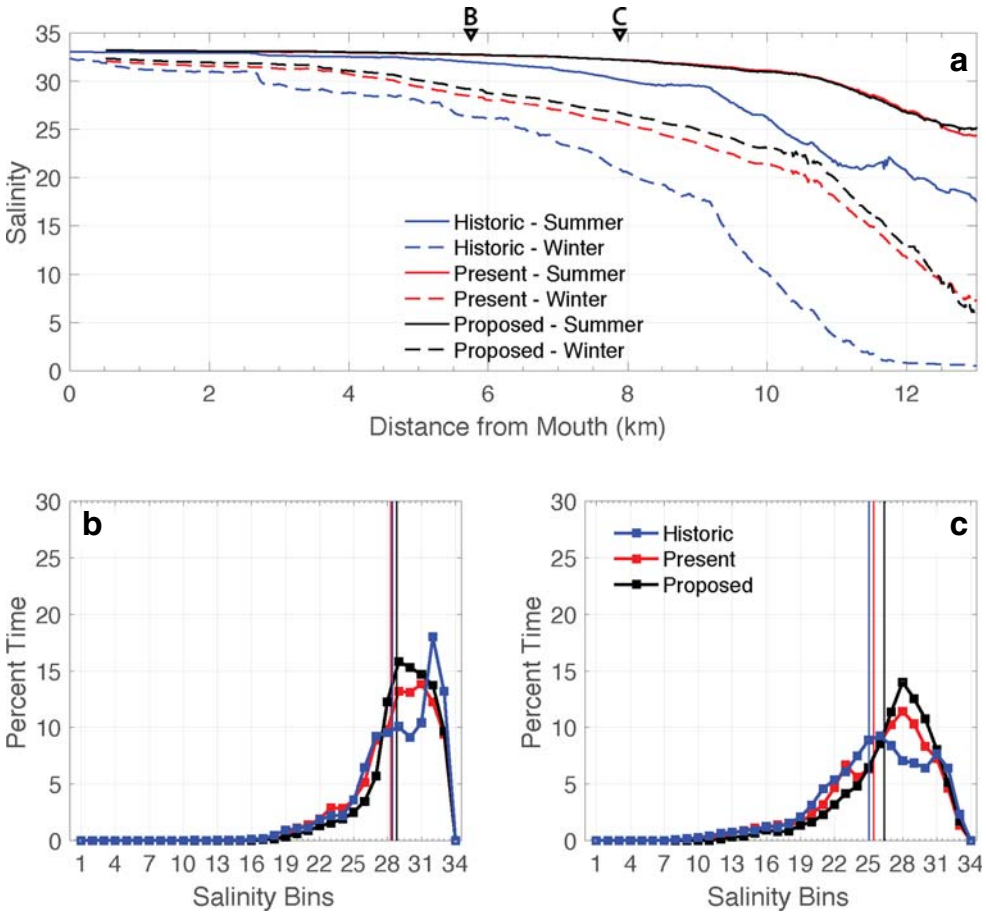

Fig. 8 (a) Time-averaged bottom salinity along a thalweg transect going from the estuary mouth up South Slough for the six simulated scenarios. Triangles indicate locations for panels (B) and (C). (b) Percent time within a certain salinity class for only the winter high-flow scenario at the along-estuary location (5.5 km) indicated in A for each bathymetry. Solid vertical lines show the mean salinity for each bathymetry (color) at that location. (c) Same as in (b), but for a location 8 km along estuary, as indicated in panel (a)

industrial centers. In estuaries on the US East Coast, many land reclamation projects began in the early 1800s and then accelerated due to the advent of railways, followed by increasing urbanization and then the development of airports. In the late 1800s, these changes were accompanied by major dredging projects facilitated by steam engine technology (Nichols and Howard-Strobel 1991; Talke et al. 2018; Familkhalili and Talke 2016). In Coos Bay, entrance modification began in the late 1800s to facilitate ship traffic, and major land reclamation began around 1910 and continued at a steady pace until 1970. A succession of projects including agricultural and urban development, construction of transportation infrastructure, channel modification for ship traffic, and intertidal reclamation reduced the area of the estuary by ~0.19% (relative to the 1865 area) each year between 1910 and 1970, with a disproportionate loss of shallow areas common to many systems modified in the past 150–200 years (Figs. 2 and 3; Ivy 2015; Nichols and Howard-Strobel 1991; Lotze 2010; Chant et al. 2018; Talke et al. 2018). Many of these changes were accompanied by shoreline hardening, e.g., placement of rip-rap for the airport runway, Charleston Harbor, and North Bend and Coos Bay waterfronts (Fig. 2).

Bathymetric changes were primarily driven by progressive channel deepening and dumping of dredge spoils in intertidal and shallow subtidal areas (Figs. 2, 3). These paired activities amplify the disproportionate shift of estuarine volumes to greater depths, i.e., deepening of the hypsometric curve for the estuary (Fig. 3B). This effect is common in many estuaries, since dredge spoils are often desirable for creation of new land for agricultural and industrial uses, and transporting spoils far from the dredging site is costly (e.g., Nichols and Howard-Strobel 1991). This shift impacts not only the distribution of subaqueous habitats but also the hydrodynamics of the system ("Implications for Estuarine Processes" and "Forecasted Changes in Response to Dredging" sections), as exemplified by the model results presented here.

Similar to other modified estuaries, the volumetric changes caused by estuarine modification have far outpaced gradual effects of sea-level rise. Assuming a regional net rate of sea-level rise of 1.10 mm/year (NOAA 2018) and an estuarine area of 54 km^2, the annual volume increase due to the net effect of global and local sea-level change would be ~5.94×10^6 m^3 per century, a ~3–4% increase over the present volume. The actual increase has probably been smaller, due to sedimentation.

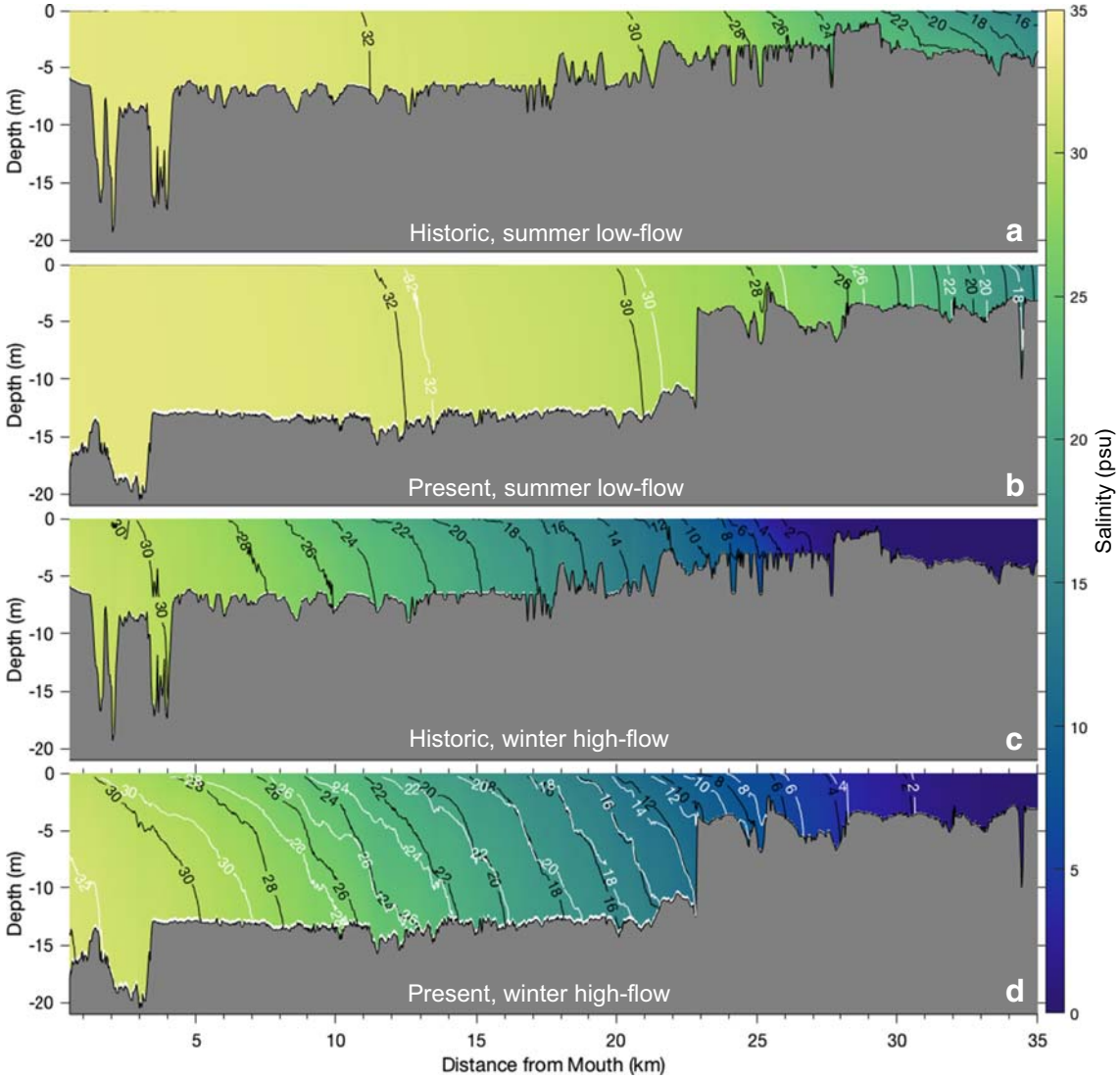

Fig. 9 (a) Time-averaged salinity along a thalweg transect going from the estuary mouth up the Coos River for summer low-flow conditions and historical bathymetry. Salinity contour intervals (black) are set to 2. (b) Same as (a), but for the present-day bathymetry (color and black contours). For comparison, the white contours show the simulated salinity field using the proposed dredging bathymetry (not shown) using the same contour interval. (c) Same as in (a) but for winter high-flow conditions and historical bathymetry. (d) Same as in (b) but for winter high-flow conditions

Johnson et al. (2019) note sediment-accumulation rates similar to rates of sea-level rise on shallow flats in Haynes Inlet and South Slough, and the navigation channel is routinely dredged to clear accumulated sediments, suggesting active sedimentation. Even without accounting for infilling by sedimentation, this calculated 3–4% per century volume increase due to sea-level rise is small relative to the 21% increase in volume that has occurred since 1865 (amounting to ~ 14% per century).

Implications for Estuarine Processes

The increase in estuarine volume, deepening of the main channel, and expansion of the estuary entrance have allowed a greater volume of saltwater to propagate into the estuary during all tidal and freshwater discharge conditions. The major effects are an overall increase in tidal amplitude, increase in salinity intrusion, and weaker but more ebb-dominant currents.

The increased tidal amplitude between the historical and modern cases is consistent with changes observed and modeled in other estuaries, including in the Delaware (DiLorenzo et al. 1993), Ems (Winterwerp et al. 2013), Columbia (Jay et al. 2011), Cape Fear (Familkhalili and Talke 2016), and Hudson (Ralston et al. 2019) estuaries. The deepening with dredging and narrowing with land reclamation of the Coos Estuary both tend to increase tidal amplitude (Friedrichs and Aubrey 1994). Deepening reduces the

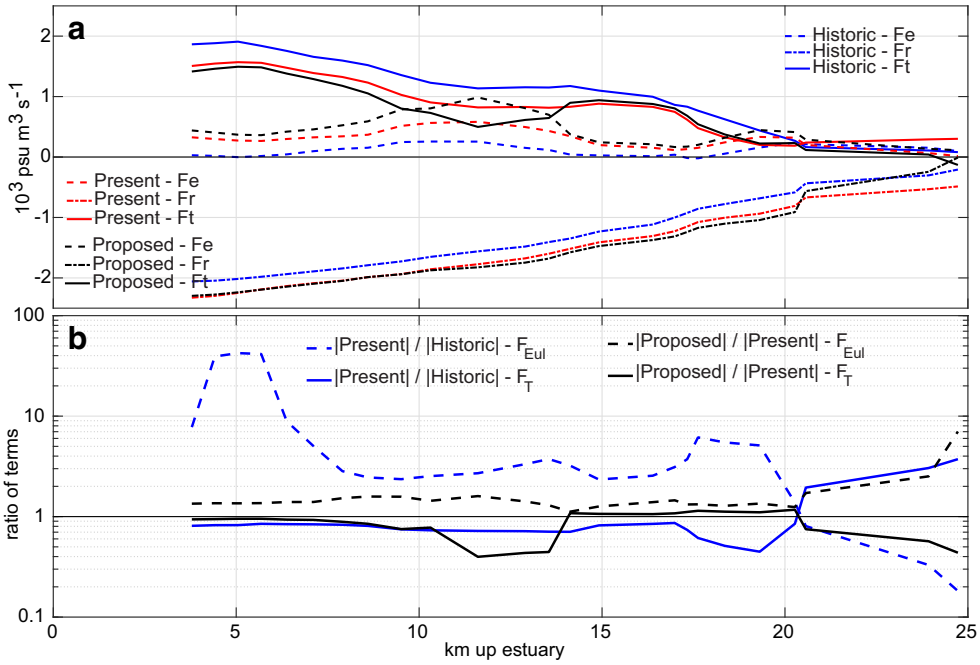

Fig. 10 (a) Components of the salt flux decomposition for the average winter case for each geometry (color), including the tidal salt flux (F_T), gravitational salt flux (F_{Eul}), and river salt flux (F_R). Positive values indicate flux of salt into the estuary. (b) Ratio of terms to compare the magnitude of F_T and F_{Eul} in the present-day geometry to the historical and proposed cases. Note the log scale on the y-axis

influence of friction on reducing the tide, and narrowing enhances the effect of convergence on amplifying the tide. In the historical case, friction dominated near the mouth and decreased the tidal amplitude in the lower estuary, but above about 10 km, convergence amplified it as the channel narrowed (Fig. 6a). In the modern case, the increase in depth and decrease in velocity reduce the frictional losses such that the tide increases continuously over the lower 20 km.

Despite the increase in tidal amplitude, the tidal velocities in the estuary have decreased because the cross-sectional area has increased with channel deepening. Similarly, the increase in mean channel depth (<h>, ~50–100% increase) is proportionally greater than the increase in tidal amplitude (a, ~30% increases) so that the ratio a/<h> has decreased between historical and modern configurations. This ratio represents the tidal nonlinearity in water depth, and larger ratios result in

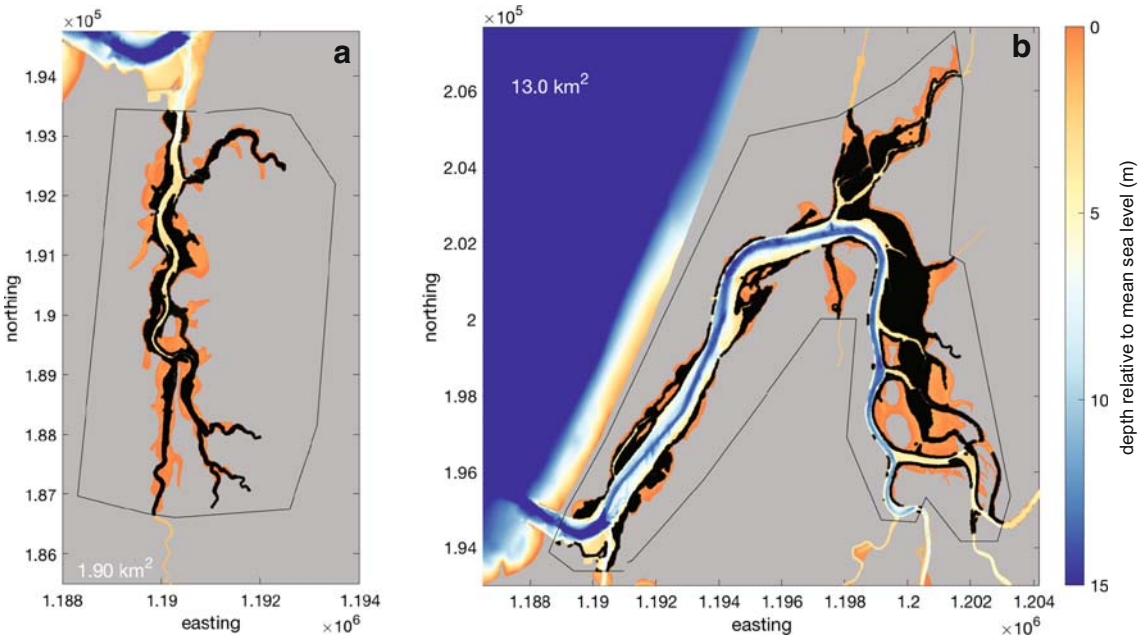

Fig. 11 Potential eelgrass habitat areas, as identified by the regions 0.5 m above and 1.0 m below MLLW. (a) South Slough. (b) Main estuary. Potential habitat is shaded black. Polygons denote the region of the bathymetric dataset that were considered. MLLW was referenced to MSL based on the Charleston datum for South Slough and the North Bend datum for the main estuary, as described in the "Characterizations of Suitable Habitat" section

more flood-dominant velocities (Friedrichs and Aubrey 1994). In contrast, tidal variation in width (Δb) relative to the average width (b) is large for the Coos Estuary, and ebb dominance increases as the ratio $\Delta b/b$ increases. The increased ebb dominance in the modern model indicates that the effect of increased channel depth (relative to the change in tidal amplitude), which tends to reduce flood dominance, has outweighed the effect of the reduction in intertidal area, which would tend to decrease the ebb dominance.

Saltwater propagates farther landward for the modern bathymetry than the historical, with greater differences between cases for winter high-discharge forcing than for summer low-flow. An increase in salinity intrusion in the modern conditions compared with historical has also been noted in modeling studies of the Tampa Bay (Meyers et al. 2014), San Francisco (Andrews et al. 2017), and Hudson (Ralston and Geyer 2019) estuaries. Locally, theory suggests that an increase in channel depth increases both the estuarine circulation and residual stratification, resulting in a nonlinear increase in subtidal salt flux and landward expansion of the salinity field (MacCready and Geyer 2010). While subtidal processes dominate the salt flux in many estuaries, the tidal salt flux provides the primary mechanism of exchange in the present-day geometry of the Coos Estuary (Conroy et al. 2019). Historically, the tidal salt flux was even more dominant, due to weaker estuarine circulation and residual stratification for a shallower channel and a much smaller F_{Eul} term (Fig. 10). The tidal salt flux scales with tidal velocities in the modern system (Conroy et al. 2019), so the greater F_T term in the historical bathymetry case is consistent with its stronger tidal velocities. In the future proposed dredging case, the magnitude of the gravitational circulation increases and steady salt flux becomes similar to the tidal salt flux term (Fig. 10). These changes suggest that a deepening of the channel by dredging increases the salt flux and increases the length of the salt intrusion (Figs. 8, 9).

Theory for an estuary where the steady term dominates the salt flux suggests that at equilibrium, the salinity intrusion length scales approximately with H^2 (MacCready and Geyer 2010). For an estuary where the tidal diffusive term dominates, the salinity intrusion scales with H, assuming that the tidal diffusivity does not also depend on depth. In the Coos Estuary, the average channel depth increased by roughly 70% averaged over the lower 25 km between the historical and modern cases, while the length of the salinity intrusion increased by about 20% (Figs. 7–9). Similarly, the depth increase from the modern system to the proposed dredging case is about 7%, but the increase in the salinity intrusion is more modest, about 1%. This relative insensitivity of the length of the salinity intrusion to estuary depth is in part reflects the dominance of the tidal salt flux, but as the system gets deeper and the steady salt flux term increases in importance, the geometric constraints of basin size limit the expansion of the salinity distribution farther landward. Dredging also occurred predominantly in the lower 20 km of the estuary, so as the salinity intrusion expands landward of the dredged region, the changes in bathymetry and salt flux processes were more modest. Similar results were found for Kill van Kull and Newark Bay (NJ), where extensive deepening of a channel for navigation increased the estuarine circulation in the lower estuary, but landward expansion of the salinity intrusion was limited by basin size constraints (Chant et al. 2018).

Forecasted Changes in Response to Dredging

The proposed dredging project would improve access for vessels to the Jordan Cove terminal and would involve deepening the western navigation channel from ~ 11 to 14 m and widening it by ~ 50%. This change would increase the entrance cross-section by ~ 2–9% (Fig. S4) and increase the total volume of the estuary by ~ 3.3%. In terms of volume, this proposed change is on par with about a century of sea-level rise (3–4% increase in volume, given present rates of sea-level rise). Impacts on tides and currents are forecasted to be relatively minor, however. The shift in tidal amplitude is negligible (Fig. 6a). Current speeds and ebb dominance are expected to be nearly identical to the modern case (Fig. 6b, c).

Despite the minimal impacts of proposed dredging on tides and currents, salinities are expected to change, especially for winter high-discharge conditions. Salinity gradients are forecasted to translate up-estuary in both the main channel and South Slough (Figs. 7a, 8a), and the steady component of the salt flux is expected to increase, for similar reasons as the shift between historical and modern cases. Near-bed conditions in the middle estuary (location C in Fig. 7) are expected to have longer periods with salinities > 18 psu, meaning oyster habitats between 15- and 20-km up-estuary would see greater mean salinities.

Management Applications of Mapping and Modeling Efforts

The large-scale shoreline and depth changes in estuaries worldwide over the past 150–200 years highlight the need for up-to-date bathymetric products, as tools in managing estuarine resources. In the Coos Bay example, channel dredging accompanied by decreases in total area (similar to many systems worldwide) has changed the hydrodynamics and salt propagation in the estuary, but these changes can only be accurately assessed using models that account for shifts in both deep and shallow portions of the estuary. The latter are difficult to map since they lie above the navigable depth for most vessels, and thus novel methods must be used. In this study, airborne water-penetrating lidar, single-beam personal watercraft surveys, and existing NOAA bathymetric data were

successfully merged and used to drive the hydrodynamic model (see also Conroy et al. 2019).

These datasets have been rapidly adapted by coastal managers and stakeholders in management of the estuary and in planning future development and restoration projects (Table 2). Bathymetric data have been incorporated by state agencies into updated Coastal and Marine Ecological Classification Standard (CMECS) habitat maps, which are in turn used by local government managers, planners, and restoration practitioners. The bathymetric data are also being incorporated into an updated estuarine management plan by local city and county governments, used by non-profit groups looking at blue carbon components to mitigation and restoration work, used by agencies and contractors responsible for assessing the potential impacts of proposed channel modifications, and used by the South Slough NERR to inform restoration projects.

An ongoing specific application of these data relates to restoration of eelgrass (*Zostera marina*). This species has declined estuary-wide since the 1970s, and severe declines were seen in the South Slough arm of the estuary in 2016 with complete loss at many sites by 2018 (A. Helms, personal communication). *Zostera marina* is considered an essential fish habitat and a habitat area of particular concern by NOAA due to its susceptibilities to human-caused disturbance and water quality conditions. The South Slough NERR is now using the bathymetric data to identify potential suitable eelgrass habitat by delineating depths where highest densities occur (Thom et al. 2008; Fig. 11). Because these habitats typically occur in shallow and intertidal regions, merging lidar and personal watercraft survey data have been critical to providing a useful tool for this system.

South Slough NERR also plans to use data products from this study to inform native Olympia oyster (*Ostrea lurida*) restoration by determining hydrodynamic connectivity of larvae between oyster beds and likely settlement sites of invasive green crabs (*Carcinus maenas*). Analyses of future salinity distributions can also inform managers of whether or not future dredging may impact the ideal salinity range for oyster cultures. For example, during wintertime high-flow periods, the time-averaged 25-psu isohaline is forecasted to shift upestuary from ~8–12 to ~8–14 km (Fig. 9d) as a result of dredging, and regions near ~19 km (where oyster beds are located) are expected to be exposed to waters of 18–26 psu for up to 4% more time (Fig. 7c). Together, these examples highlight the utility of the bathymetric data and associated hydrodynamic models in providing useful information for local ecologists and stakeholders.

Conclusions

Based on analyses of historical maps from the past 150 years, the Coos Bay Estuary has undergone diverse developments and system changes common to many larger estuaries worldwide. Since 1865, the total estuary area has decreased by 12%, and the estuary volume has increased by 21%. Most of the area loss occurred between ~1910 and 1970 during the construction of airport, railroad, and shipping facilities and disposal of dredge spoils within the estuary. Channel dredging and spoil disposal in shallow areas resulted in a disproportionate increase of estuarine volume in deeper portions of the estuary, an effect common in many developed estuaries. Together, these changes have altered the distribution of subaqueous habitats and impacted the tides, currents, and salinity distribution in the system.

Data from the historical map analyses and updated bathymetry were combined and used to drive a hydrodynamic model, in order to provide an additional management tool demonstrating historical and forecasted changes to tides, currents, and salinity in the estuary. Channel deepening between 1865

Table 2 List of known current users of the bathymetric data produced by this study with brief purpose and management implications

	Name/affiliation	Purpose and implications
State	Department of Land Conservation and Development	*CMECS*[a] *habitat mapping*: inform updated inventories for future estuarine management plans
	Department of Geology and Mineral Industries	*Tsunami modeling*: to update plans for Cascadia earthquake tsunami inundation maps
	Department of Fish and Wildlife	*SEACOR*[b]: assess shellfish habitats and recreational fisheries in estuary
	Department of Environmental Quality	*Oil spill response planning*: run simulations to update predictions of oil spill contamination
Federal	South Slough NERR	*Eelgrass recovery plan*: loss of eelgrass beds over last the 2 years led to recovery plan development
Private	Institute for Applied Ecology	*Blue carbon feasibility*: can restoration areas in the estuary be used to finance mitigation projects
	Moffat and Nichol consultants	*Hydrodynamic modeling*: test sensitivity of estuary to proposed dredging for Jordan Cove LNG project[c]

[a] Coastal and Marine Ecological Classification Standard, https://www.oregon.gov/lcd/ocmp

[b] Shellfish and Estuarine Assessment of Coastal Oregon: https://www.dfw.state.or.us/mrp/shellfish/seacor/

[c] Proposed Liquid Natural Gas terminal. https://www.jordancovelng.com/project

and present resulted in weaker but more ebb-dominant currents, an increase in tidal amplitude, and an ~ 18% increase in the salinity intrusion length. The increased salinity is associated with a doubling of the subtidal, gravitational circulation salt flux such that the contribution to the total salt flux of tidal dispersive component decreases from 80 to 60%. A future proposed channel deepening project would increase the primary channel depth from ~ 11 to 14 m, resulting in a ~ 3.3% increase in estuarine volume—roughly equivalent to a century of sea-level rise at present rates (assuming no sedimentation). Model simulations forecast little impact on tidal amplitude and currents, though the salinity intrusion is expected to propagate an additional ~ 2–5-km up-estuary and the steady salt flux to increase by an additional 50–100%.

This study illustrates the value of leveraging existing and new bathymetric data, historical charts, and modern hydrodynamic models to provide dynamic tools for local managers, e.g., an interdisciplinary connection with managers at the South Slough National Estuarine Research Reserve, state agencies, and private consultants, made through modeling efforts and good communication with stakeholders. While modern high-resolution bathymetry is an asset in itself, converting it into a modeling framework provides a greatly expanded and dynamic tool for evaluating past and future changes in estuarine function.

Acknowledgments Computations were performed on the University of Oregon high-performance computer Talapas. We thank Kira Bartlett from UO for assistance in digitizing historical maps, Adam DeMarzo and Alicia Helms at SSNERR for helpful discussions about South Slough management, and the Oregon Department of Fish & Wildlife for SEACOR data. We also thank the editors and two anonymous reviewers for their constructive comments, which helped improve the manuscript.

Funding information This work was partially sponsored by the National Estuarine Research Reserve System Science Collaborative, which supports collaborative research that addresses coastal management problems important to the reserves. The Science Collaborative is funded by the National Oceanic and Atmospheric Administration and managed by the University of Michigan Water Center (NAI4NOS4190145).

References

Andrews, S.W., E.S. Gross, and P.H. Hutton. 2017. Modeling salt intrusion in the San Francisco Estuary prior to anthropogenic influence. *Continental Shelf Research* 146: 58–81. https://doi.org/10.1016/j.csr.2017.07.010.

Baker, C. 1978. A study of estuarine sedimentation in South Slough, Coos Bay, Oregon (pp. 1–118). Thesis, Portland State University.

Baptista, A.M. 1989. *Salinity in Coos Bay, Oregon: review of historical data (1930–1989). Report ESE–89–001*. Portland: U.S. Army Engineer District.

Barbier, E.B., S.D. Hacker, C. Kennedy, E.W. Koch, A.C. Stier, and B.R. Silliman. 2011. The value of estuarine and coastal ecosystem services. *Ecological Monographs* 81 (2): 169–193. https://doi.org/10.1890/10-1510.1.

Bartlett, K. 2018. *Shoreline change in the Coos Bay estuary. University of Oregon senior thesis*. Eugene: Department of Earth Sciences.

Borde, A.B., R.M. Thom, S. Rumrill, and L.M. Miller. 2003. Geospatial habitat change analysis in Pacific Northwest coastal estuaries. *Estuaries* 26 (4): 1104–1116. https://doi.org/10.1007/BF02803367.

Brophy, L. 2017. Indirect assessment of west coast USA tidal wetland loss. File geodatabase feature class, Pacific Marine and Estuarine Fish Habitat Partnership. https://www.pacificfishhabitat.org/data/tidal-wetlands-lossassessment/. Accessed 06 April 2020.

Caldera, M. 1995. *South Slough adventures: life on a Southern Oregon Estuary*. Coos Bay: Friends of South Slough, South Coast Printing Company.

Carignan, K.S., Taylor, L.A., Eakins, B.W., Warnken, R.R., Sazonova, T., & Schoolcraft, D.S. 2009. Digital elevation model of Port Orford, Oregon: procedures, data sources, and analysis. NOAA Tech. Mem. NESDIS NGDC-21. 38 pp.

Chant, R.J., Sommerfield, C.K., & Talke, S.A. 2018. Impact of channel deepening on tidal and gravitational circulation in a highly engineered Estuarine Basin, 1–14. https://doi.org/10.1007/s12237-018-0379-6

Chen, C., H. Liu, and R.C. Beardsley. 2003. An unstructured grid, finite-volume, three-dimensional, primitive equations ocean model: application to coastal ocean and estuaries. *Journal of Physical Oceanography* 20: 159–186.

Conroy, T., D.A. Sutherland, and D.K. Ralston. 2019. Estuarine exchange flow variability in a seasonal, segmented estuary. *Journal of Physical Oceanography* 50:595–613.

DiLorenzo, J.L., P. Huang, M.L. Thatcher, and T.O. Najarian. 1993. Dredging impacts of Delaware estuary tides, Estuarine and Coastal Modeling III: Proceedings of the 3rd International Conference, 86−104. Eatontown: ASCE.

Egbert, G.D., and S.Y. Erofeeva. 2002. Efficient inverse modeling of barotropic ocean tides. *Journal of Atmospheric and Oceanic Technology* 19 (2): 183–204.

Familkhalili, R., & Talke, S.A. 2016. The effect of channel deepening on tides and storm surge: a case study of Wilmington, NC, 1–10. https://doi.org/10.1002/2016GL06949410.1002/(ISSN)1944-8007.

Fischer, H.B. 1976. Mixing and dispersion in estuaries. *Annual Review of Fluid Mechanics* 8 (1): 107–133.

Friedrichs, C.T., and D.G. Aubrey. 1994. Tidal propagation in strongly convergent channels. *Journal of Geophysical Research, Oceans* 99: 3321–3336. https://doi.org/10.1029/93JC03219.

Giddings, S.N., P. MacCready, B.M. Hickey, N.S. Banas, K.A. Davis, S.A. Siedlecki, V.L. Trainer, R.M. Kudela, N.A. Pelland, and T.P. Connolly. 2014. Hindcasts of potential harmful algal bloom transport pathways on the Pacific Northwest coast. *Journal of Geophysical Research, Oceans* 119 (4): 2439–2461.

Groth, S., and S. Rumrill. 2009. History of Olympia oysters (Ostrea lurida Carpenter 1864) in Oregon estuaries, and a description of recovering populations in Coos Bay. *Journal of Shellfish Research* 28 (1): 51–58. https://doi.org/10.2983/035.028.0111.

Guerry, A.D., M.H. Ruckelshaus, K.K. Arkema, J.R. Bernhardt, G. Guannel, C.-K. Kim, M. Marsik, M. Papenfus, J.E. Toft, G. Verutes, S.A. Wood, M. Beck, F. Chan, K.M.A. Chan, G. Gelfenbaum, B.D. Gold, B.S. Halpern, W.B. Labiosa, S.E. Lester, P.S. Levin, M. McField, M.L. Pinsky, M. Plummer, S. Polasky, P. Ruggiero, D.A. Sutherland, H. Tallis, A. Day, and J. Spencer. 2012. Modeling benefits from nature: using ecosystem services to inform coastal and marine spatial planning. *International Journal of Biodiversity Science, Ecosystem Services & Management*. https://doi.org/10.1080/21513732.2011.647835.

Hansen, D.V., and M. Rattray Jr. 1965. Gravitational circulation in straits and estuaries. *Journal of Marine Research* 23: 104–122.

Hansen, D.V., and M. Rattray Jr. 1966. New dimensions in estuary classification. *Limnology and Oceanography* 11: 319–326.

Hickey, B.M., and N.S. Banas. 2003. Oceanography of the US Pacific Northwest coastal ocean and estuaries with application to coastal ecology. *Estuaries* 26 (4): 1010–1031.

Hoffnagle, J., and R. Olson. 1974. *Salt marshes of the Coos Bay Estuary*. Charleston: Oregon Institute of Marine Biology.

Ivy, D. 2015. A brief overview of the Coos Bay Area's economic and cultural history. In *Communities, Lands & Waterways Data Source*, ed. C.E. Cornu and J. Souder. Coos Bay: Partnership for Coastal Watersheds, South Slough National Estuarine Research Reserve, and Coos Watershed Association.

Jakobsson, M., A. Armstrong, B.R. Calder, L.C. Huff, and L.A. Mayer. 2005. On the use of historical bathymetric data to determine changes in bathymetry: an analysis of errors and application to Great Bay Estuary, New Hampshire. *International Hydrographic Review* 6 (3): 25–41.

Jay, D.A., K. Leffler, and S. Degens. 2011. Long-term evolution of Columbia River tides. *Journal of Waterway, Port, Coastal, and Ocean Engineering* 137: 182–191. https://doi.org/10.1061/(ASCE)WW.1943-5460.0000082.

Johnson, G.M., D.A. Sutherland, J.J. Roering, N. Mathabane, and D.G. Gavin. 2019. Estuarine dissolved oxygen inferred from sedimentary trace metal and organic matter preservation in Coos Bay, Oregon, USA. *Estuaries and Coasts* 42 (5): 1211–1225. https://doi.org/10.1007/s12237-019-00580-8.

Komar, P.D., J.C. Allan, and P. Ruggiero. 2011. Sea level variations along the U.S. Pacific Northwest Coast: tectonic and climate controls. *Journal of Coastal Research* 276: 808–823. https://doi.org/10.2112/JCOASTRES-D-10-00116.1.

Lane, A. 2004. Bathymetric evolution of the Mersey estuary, UK, 1906–1997: causes and effects. *Estuarine, Coastal and Shelf Science* 59 (2): 249–263. https://doi.org/10.1016/j.ecss.2003.09.003.

Lerczak, J.A., W.R. Geyer, and R.J. Chant. 2006. Mechanisms driving the time-dependent salt flux in a partially stratified estuary. *Journal of Physical Oceanography* 36 (12): 2296–2311.

Lotze, H. 2010. Historical reconstruction of human-induced changes in U.S. estuaries. In *Oceanography and marine biology - an annual review*, vol. 20103650, 2nd ed., 267–338. CRC Press. https://doi.org/10.1201/ebk1439821169-c5.

MacCready, P., and W.R. Geyer. 2010. Advances in estuarine physics. *Annual Review of Marine Science* 2: 35–58. https://doi.org/10.1146/annurev-marine-120308-081015.

Martínez, M.L., A. Intralawan, G. Vázquez, O. Pérez-Maqueo, P. Sutton, and R. Landgrave. 2007. The coasts of our world: ecological, economic and social importance. *Ecological Economics* 63 (2–3): 254–272. https://doi.org/10.1016/j.ecolecon.2006.10.022.

Meyers, S.D., A.J. Linville, and M.E. Luther. 2014. Alteration of residual circulation due to large-scale infrastructure in a coastal plain estuary. *Estuaries and Coasts* 37 (2): 493–507. https://doi.org/10.1007/s12237-013-9691-3.

Nichols, M.M., and M.M. Howard-Strobel. 1991. Evolution of an urban estuarine harbor: Norfolk, Virginia. *Journal of Coastal Research* 7 (3): 745–757.

Nidzieko, N.J., and D.K. Ralston. 2012. Tidal asymmetry and velocity skew over tidal flats and shallow channels within a macrotidal river delta. *Journal of Geophysical Research* 117 (C3): 1–17. https://doi.org/10.1029/2011JC007384.

NOAA (National Oceanic and Atmospheric Administration). (2018). Relative Sea Level Trend 9432780 Charleston, Oregon. https://tidesandcurrents.noaa.gov/sltrends/sltrends_station.shtml?id=9432780. Revised 08 Aug, 2018. Accessed 29 Mar, 2019.

NOAA (National Oceanic and Atmospheric Administration). (2019a). Datums for 9432895, North Bend, Coos Bay OR, https://tidesandcurrents.noaa.gov/datums.html?id=9432895, accessed 28 Mar, 2019.

NOAA (National Oceanic and Atmospheric Administration). (2019b). Office of Coast Survey Historical Map & Chart Collection, https://historicalhistoricalcharts.noaa.gov, accessed 22 Mar 2019.

OCMP (Oregon Coastal Management Program). (2014). CMECS Estuarine Substrate Component v.0.4, OCMP, 2014. Vector digital data. Available at https://www.coastalatlas.net/metadata/CMECS_Substrate_Component_OCMP_2014.html. Accessed 1 Apr 2019.

Pawlowicz, R., B. Beardsley, and S. Lentz. 2002. Classical tidal harmonic analysis including error estimates in MATLAB using T_TIDE. *Computers and Geosciences* 28: 929–937.

Ralston, D.K., and W.R. Geyer. 2019. Response of the salinity intrusion, estuarine circulation, and stratification to channel deepening in an urbanized estuary. *Journal of Geophysical Research, Oceans*. https://doi.org/10.1029/2019JC015006.

Ralston, D.K., W.R. Geyer, and J.A. Lerczak. 2010. Structure, variability, and salt flux in a strongly forced salt wedge estuary. *Journal of Geophysical Research, Oceans*. https://doi.org/10.1029/2009JC005806..

Ralston, D.K., S. Talke, W.R. Geyer, H.A. Al-Zubaidi, and C.K. Sommerfield. 2019. Bigger tides, less flooding: effects of dredging on barotropic dynamics in a highly modified estuary. *Journal of Geophysical Research, Oceans* 124 (1): 196–211.

Roye, C. 1979. *Natural resources of Coos Bay estuary. Estuary Inventory Report*. Portland: Oregon Department of Fish and Wildlife 87 pp.

Ruggiero, P., G.A. Kaminsky, G. Gelfenbaum, and B. Voigt. 2005. Seasonal to interannual morphodynamics along a high-energy dissipative littoral cell. *Journal of Coastal Research* 21: 553–578.

Rumrill, S.S. 2006. *The ecology of the South Slough estuary: Site profile of the South Slough National Estuarine Research Reserve*. Charleston: South Slough National Estuarine Research Reserve 238 pp.

Satake, K., K.L. Wang, and B.F. Atwater. 2003. Fault slip and seismic moment of the 1700 Cascadia earthquake inferred from Japanese tsunami descriptions. *Journal of Geophysical Research* 108: 2523. https://doi.org/10.1029/2003JB002521.

Sutherland, D.A., and M.A. O'Neill. 2016. Hydrographic and dissolved oxygen variability in a seasonal Pacific Northwest estuary. *Estuarine, Coastal and Shelf Science* 172 (C): 47–59. https://doi.org/10.1016/j.ecss.2016.01.042.

Talke, S.A., H.E. de Swart, and H.M. Schuttelaars. 2009. Feedback between residual circulations and sediment distribution in highly turbid estuaries: an analytical model. *Continental Shelf Research* 29 (1): 119–135. https://doi.org/10.1016/j.csr.2007.09.002.

Talke, S.A., A.C. Kemp, and J. Woodruff. 2018. Relative Sea level, tides, and extreme water levels in Boston Harbor from 1825 to 2018. *Journal of Geophysical Research, Oceans* 123 (6): 3895–3914. https://doi.org/10.1029/2017JC013645.

Thom, R.M., S.L. Southard, A.B. Borde, and P. Stoltz. 2008. Light requirements for growth and survival of eelgrass (Zostera marina L.) in Pacific Northwest (USA) estuaries. *Estuaries and Coasts* 31 (5): 969–980.

Umlauf, L., and H. Burchard. 2003. A generic length-scale equation for geophysical turbulence models. *Journal of Marine Research* 61: 235–265.

van der Wal, D., K. Pye, and A. Neal. 2002. Long-term morphological change in the Ribble estuary, Northwest England. *Marine Geology* 189 (3–4): 249–266. https://doi.org/10.1016/S0025-3227(02)00476-0.

Van Dyke, E., and K. Wasson. 2005. Historical ecology of a Central California estuary: 150 years of habitat change. *Estuaries* 28 (2): 173–189. https://doi.org/10.1007/BF02732853.

van Maren, D.S., T. van Kessel, K. Cronin, and L. Sittoni. 2015. The impact of channel deepening and dredging on estuarine sediment concentration. *Continental Shelf Research* 95 (C): 1–14. https://doi.org/10.1016/j.csr.2014.12.010.

Winterwerp, J.C., Z.B. Wang, A. van Braeckel, G. van Holland, and F. Kösters. 2013. Man-induced regime shifts in small estuaries—II: a comparison of rivers. *Ocean Dynamics* 63 (11–12): 1293–1306. https://doi.org/10.1007/s10236-013-0663-8.